Continuous time resource selection analysis for moving animals

Y. Wang[1], P.G. Blackwell[1], J.A. Merkle[2] and J.R. Potts[1*]

[1] School of Mathematics and Statistics, University of Sheffield, Hicks Building, Hounsfield Road, Sheffield

S3 7RH, UK

[2] Wyoming Cooperative Research Unit and Department of Zoology and Physiology, University of Wyoming,

Laramie, WY, USA

* Correspondence: E-mail: j.potts@sheffield.ac.uk

Short title: Continuous time resource selection analysis

Word Count: 7000

Abstract

1. Resource selection analysis (RSA) seeks to understand how spatial abundance covaries with environmental features. By combining RSA with movement, step selection analysis (SSA) has helped uncover the mechanisms behind animal relocations, thereby giving insight into the movement decisions underlying spatial patterns. However, SSA typically assumes that at each observed location, an animal makes a 'selection' of the next observed location. This conflates observation with behavioural mechanism and does not account for decisions occurring at any other time along the animal's path.

2. To address this, we introduce a continuous time framework for resource selection. It is based on a switching Ornstein-Uhlenbeck (OU) model, parameterised by Bayesian Monte Carlo techniques. Such OU models have been used successfully to identify switches in movement behaviour, but hitherto not combined with resource selection. We test our inference procedure on simulated paths, representing both migratory movement (where landscape quality varies according to season) and foraging with depletion and renewal of resources (where the variation is due to past locations of the animals). We apply our framework to location data of migrating mule deer (*Odocoileus hemionus*) to shed light on the drivers of migratory decisions.

3. In a wide variety of simulated situations, our inference procedure returns reliable estimations of the parameter values, including the extent to which animals trade-off resource quality and travel distance (within 95% posterior intervals for the vast majority of cases). When applied to the mule deer data, our model reveals some individual variation in parameter values. Nevertheless, the migratory decisions of most individuals are well-described by a model that accounts for the cost of moving and the difference between instantaneous change of vegetation quality at source and target patches.

4. We have introduced a technique for inferring the resource-driven decisions behind animal movement that accounts for the fact that these decisions may take place at any point along a path, not just when the animal's location is known. This removes an oft-acknowledged but hitherto little-addressed shortcoming of stepwise movement models. Our work is of key importance in understanding how environmental features drive movement decisions and, as a consequence, space use patterns.

1   Introduction

Resource selection is a fundamental tool for understanding the drivers behind spatial distributions of animals (Manly *et al.* (2002)). Applications not only include estimation of the distribution and abundance of species, but also prediction of species diversity, representation of interactions of species, and

identification of key spatial features of the landscape (e.g. Chetkiewicz & Boyce (2009), Lendrum *et al.* (2012), Boyce (2006), McLoughlin *et al.* (2010)). Furthermore, the role of movement as a primary cause of spatial patterning is becoming increasingly evident (Cagnacci *et al.* (2010), Thurfjell *et al.* (2014)) and formally integrated into the resource selection framework (Moorcroft & Barnett (2008), Avgar *et al.* (2016)). This has diverse applications including home range formation (Merkle *et al.* (2017)), competition (Vanak *et al.* (2013)), disease spread (Merkle *et al.* (2018)), territorial interactions (Potts *et al.* (2014b)), and predator-prey dynamics (Bastille-Rousseau *et al.* (2015)).

Step Selection Analysis (SSA) has provided the main tool for incorporating movement into resource selection (Fortin *et al.* (2005), Forester *et al.* (2009), Thurfjell *et al.* (2014)). It relies on comparing movement between two successive location fixes (called a 'step') with various possible steps potentially available to the animal. As well as explicitly incorporating movement into the resource selection framework, SSA has recently been extended to estimate movement and resource selection parameters simultaneously, termed integrated step selection analysis (iSSA; Avgar *et al.* (2016)). The iSSA procedure corrects for any error implicit in the choice of distribution for 'available' steps, and can be used to parameterise a mechanistic model of animal movement. In addition, appropriate modelling of resource selection at the level of the individual step can link it to the long-term utilisation distribution (Michelot *et al.* (2018)).

However, both SSA and iSSA implicitly assume that movement decisions occur on the same scale as the observation frequency (McClintock *et al.* (2014)), or the scale of a regular subsample of the observations (Potts *et al.* (2014c)). These assumptions may result in misleading interpretations of inferences from data, and in particular make it tricky to work with irregularly sampled data (McClintock *et al.* (2014), Thurfjell *et al.* (2014)). To avoid these issues, it makes sense to model the animal path as a continuous track, where decisions may have occurred at any point along that track, then fit this continuous-time model to the data.

Continuous-time modelling frameworks for animal movement have existed for some time. An early example is that of Blackwell (1997). There, a switching Ornstein-Uhlenbeck (OU) process was proposed, which is flexible enough to capture a wide range of animal movement patterns, and has thus gained increasing popularity over the years. It has the advantage of being amenable to rigorous and efficient parameterisation by data using Bayesian Monte Carlo methods (Blackwell (2003)) and has recently been extended to incorporate spatial heterogeneity (Harris & Blackwell (2013), Blackwell *et al.* (2016)). This opens the question as to whether it can be combined with resource selection analysis (RSA) to model animal decisions as they move in continuous time.

Several continuous-time models have already been developed to incorporate resource selection. Johnson *et al.* (2008) was one of the first such studies. This study proposed various possible models for the distribution of a location along path, conditional on the knowledge of all previous locations. However, although the models themselves were defined in continuous time, they all model movement from one

measured location to the next, so do not account for the possibility of behavioural changes between location fixes.

On the other hand, the approach of Hanks *et al.* (2015) does deal with between-observation behavioural switches. This method discretises space into a lattice and models movement as jumps between neighbouring lattice sites, building on previous work by Hooten *et al.* (2010) and Hanks *et al.* (2011). Behavioural switches are possible at any nearest-neighbour jump, not just those that correspond to measured locations. However, the implicit assumption of the model in Hanks *et al.* (2015) is that the spatial scale of discretisation represents the scale of behavioural decisions. In reality, animal movement decisions may play out on multiple scales, with localised considerations (e.g. moving around a small obstacle or over a fence) balanced with longer-term goals (e.g. moving to the next foraging patch or continuing a migratory journey). Furthermore, this technique only considers movement in response to proximate resources (e.g. a local resource gradient). In reality, animals may be attracted to resources that are quite some distance away, due to long-term memory processes. A continuous-time framework is needed that is flexible enough to account for such a variation of possibilities.

Here, we extend the switching OU framework of Blackwell *et al.* (2016) to incorporate resource selection in two separate ways. The first considers resources as objects that have an attractive pull on animals, which may take place over a considerable spatial scale (e.g. in migratory cases). If it is beneficial to move to a new area to gain access to better resources, taking into consideration the cost of moving there, then the animal becomes attracted to that area. In mathematical terms, this corresponds to a switch in the OU process. Otherwise, the animal stays in the vicinity of its current position. At any point, the best possible attractor on the landscape could switch, causing the animal to change its movement mode. We consider cases both where the landscape undergoes seasonal changes and where the quality of resources depends upon the past positions of the animal (through resource depletion and renewal).

The second modification is implemented separately from the first and takes a rather different approach to modelling animal movement. Here, rather than assuming the animal assesses the whole landscape and moves towards the most desirable goal, we assume that the animal considers only proximate aspects of the terrain and, as such, has a tendency to move up the resource gradient. This is similar to Hanks *et al.* (2015) but framed within a switching random walk framework. In doing this, the animal's path does not need to be discretised (as in Hanks *et al.* (2015)). However, by using efficient Bayesian Monte Carlo methods developed over a series of papers (Blackwell (2003), Harris & Blackwell (2013), Blackwell *et al.* (2016)), inference is still possible within a reasonable time-frame. We compare our framework with that of Hanks *et al.* (2015), testing for both speed and precision of inference by application to paths simulated from the model proposed in this paper.

We tested our modelling and inference method on both simulated and real trajectories. The simu-

lated trajectories model (a) migratory behaviour, (b) movement due to resource depletion and renewal in both patchy and lattice landscapes, and (c) resource-gradient following in a fixed (lattice) landscape. Real trajectories were measured from mule deer (*Odocoileus hemionus*) migrations in the Greater Yellowstone Ecosystem. Our simulation analysis demonstrates the ability of our method to infer parameters with reasonable accuracy. The application to mule deer data demonstrates that migratory timings may be explained by a simple trade-off between resource quality and travel distance. We include, in the Supporting Information, code for performing inference and simulating all trajectories used in this manuscript (instructions are found in Supplementary Appendix H).

2 Methods

2.1 Modelling framework

In this section, we model movements in response to the environment in two scenarios. In the first situation, we assume that animals have complete knowledge of the environment and bias their movements towards the most attractive location in space. Then we consider the other extreme, where animals only have information about local conditions.

2.1.1 Movements in response to resource change in the whole landscape

A commonly used continuous-time movement model is the OU process, which describes a biased random walk with drift towards an attraction centre. The general formalism is given as follows

$$d\mathbf{x}(t) = B(\mathbf{x}(t) - \boldsymbol{\mu}(t))dt + \Lambda d\mathbf{W}(t). \tag{1}$$

Here, $\mathbf{x}(t)$ is the animal's location at time t in n-dimensional space, $\boldsymbol{\mu}(t)$ is the attraction centre at time t, B is an n by n matrix controlling the tendency towards the attraction centre, Λ is the covariance matrix, and $\mathbf{W}(t)$ is an n-dimensional Wiener process. Under the process given by Equation (1), the probability of an animal being at location $\mathbf{x}(t + \tau)$ at time $t + \tau$, given that it was at $\mathbf{x}(t)$ at time t, is

$$\mathbf{x}(t + \tau)|\mathbf{x}(t) \sim MVN(\boldsymbol{\mu}(t) + e^{B\tau}(\mathbf{x}(t) - \boldsymbol{\mu}(t)), \Lambda - e^{B\tau}\Lambda e^{B'\tau}), \tag{2}$$

where τ is a (small) time interval and MVN stands for "Multi-variate normal".

Throughout this paper, we work in two dimensions, so that B and Λ are 2×2 matrices. Furthermore, we assume $B = -bI$ and $\Lambda = vI$ with $b, v > 0$ and I the 2×2 identity matrix, so that there is no correlation between the horizontal and vertical coordinates. Larger b leads to a stronger tendency toward the attraction centre and faster approach to the attraction centre when far away from it, while

larger v induces a wider range of wandering near the central point. Hence we refer to b as the *drift coefficient* and v the *diffusive coefficient*.

To determine the attraction centre $\boldsymbol{\mu}(t)$ in the OU process in Equation (2), a function is incorporated into our modelling framework to evaluate the attractiveness of a location or an item in space. For this, we choose a commonly used functional form known as a *resource selection function* (RSF) and defined as follows (Boyce *et al.* (2002))

$$w(\mathbf{x}) = \exp(\beta_1 z_1(\mathbf{x}) + \beta_2 z_2(\mathbf{x}) + \cdots + \beta_k z_k(\mathbf{x})), \tag{3}$$

where $\mathbf{x}$ is a location in space, $\mathbf{z}(\mathbf{x}) = (z_1(\mathbf{x}), \cdots, z_k(\mathbf{x}))$ is the vector of predictor covariates, consisting of possible factors affecting selection decision – for example, some kind of vegetation, predator pressure, distance to a road, etc. (Manly *et al.* (2002)) – and $\beta_1, \cdots, \beta_k$ are coefficients representing the relative weight of each factor. We assume that the animal has complete knowledge of the available space and decides its destination $\boldsymbol{\mu}(t)$ at time t by comparing the attractiveness of all potential target locations, given by Equation (3) (cf. Avgar *et al.* (2017)), then moves towards the most attractive destination. That is,

$$\boldsymbol{\mu}(t) = \boldsymbol{\mu}_i \qquad \text{where} \qquad w(\boldsymbol{\mu}_i) = \max_{j \in \Omega} w(\boldsymbol{\mu}_j). \tag{4}$$

Here, $\boldsymbol{\mu}_i$ is the centre of a resource unit, which may be a patch or an item, and Ω indexes the collection of all resource units, which is finite. In most typical situations, $\boldsymbol{\mu}(t)$ will be unique, because Equation (3) will normally involve continuous covariates, and so each resource unit $\boldsymbol{\mu}_j$ is likely to have a different value of $w(\boldsymbol{\mu}_j)$ associated to it. In this study, we only consider such situations, so there is never an arbitrary choice between resource units of precisely equivalent quality.

2.1.2 Movements following local resource gradient

The OU model described above assumes the animal has complete knowledge of the landscape when making a decision. At the other extreme, we might assume that the animal only has proximate knowledge of the landscape. For this, we model animals as following the local resource gradient. This can be described by a process $\mathbf{x}(t)$ satisfying a stochastic differential equation with constant drift term (Preisler *et al.* (2004))

$$d\mathbf{x}(t) = \alpha\boldsymbol{\rho}(t)dt + \boldsymbol{\Sigma}d\mathbf{W}(t), \tag{5}$$

where α is a governing the drift speed, $\boldsymbol{\rho}(t)$ is a unit vector representing the direction of drift, $\boldsymbol{\Sigma}$ is an $n \times n$ matrix controlling the diffusive aspects of movement. Here we use a two-dimensional (Euler-Maruyama) approximation of the conditional distribution of the process defined by Equation (5), which

6

168   is valid for small τ. This is given as follows

$$\mathbf{x}(t+\tau)|\mathbf{x}(t) \sim MVN(\mathbf{x}(t) + \alpha\boldsymbol{\rho}(t)\tau, \boldsymbol{\Sigma}\tau), \tag{6}$$

169   where $\mathbf{x}(t)$ is the animal's position at time t. We assume $\Sigma = \sigma^2 I$ where I the 2×2 identity matrix and

170   σ is a scalar constant. The model in Equation (6) contrasts with that of Equation (2) in that the former

171   assumes animals respond to a local resource gradient, whereas the latter models animals as choosing a

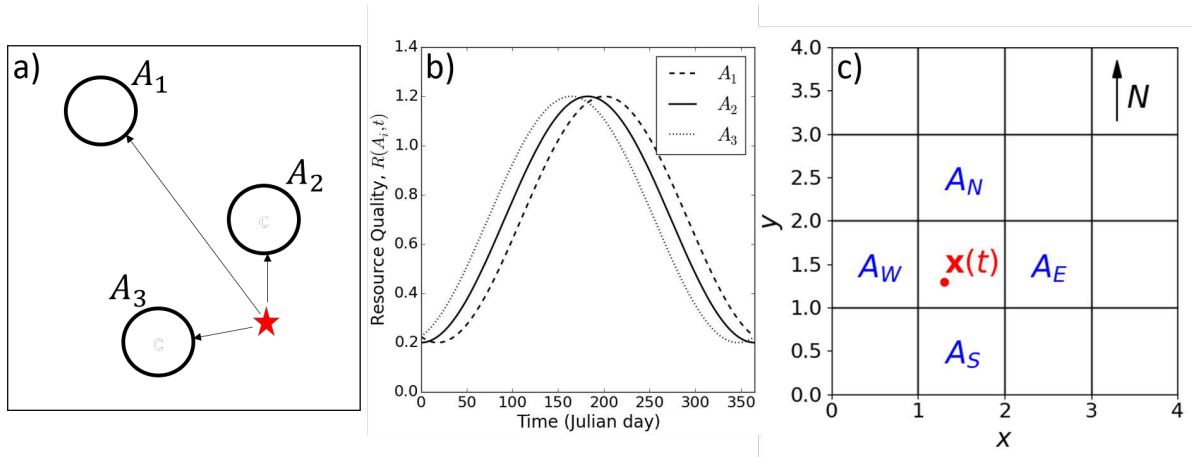172   target location from the landscape to move towards.

Figure 1: Panel (a) illustrates the patch selection model (Equations 1-4). Assume the animal is at the red star. In this simplified illustration, there are just three possible patches it can choose to move towards, A_1, A_2, and A_3 (in real situations there may be many more). The animal's choice is determined by both the patch quality, which may vary over time, and the distance to the patch. Panel (b) gives example curves of how the patch quality of each patch may vary over time, each in the format of Equation (11). Panel (c) illustrates the gradient following model (Equations 5-8). The animal is located at position $\mathbf{x}(t)$ at time t. Patches A_N, A_W, A_E and A_S are the adjacent squares to the patch where the animal is located. N, W, E, S stand for the north, west, east and south respectively. When calculating the resource gradient in the nearby area of $\mathbf{x}(t)$, the resource qualities in the four adjacent patches are considered, which means the animal only assesses resource qualities in neighbouring areas to determine its moving direction.

173   We assume that animals move in a rasterised landscape, that is, one subdivided into a square or

174   rectangular lattice. Hereafter we will consider a square lattice for simplicity. We determine the drift

175   direction $\boldsymbol{\rho}(t)$ in Equation (6) by considering the resource qualities in the four adjacent squares (North,

176   East, South, West) to the one where the animal is located. Here, the resource gradient is given as follows

177   (cf. Preisler *et al.* (2013)):

$$\nabla w(\mathbf{x}(t)) := \left(\frac{w(A_E) - w(A_W)}{\Delta x}, \frac{w(A_N) - w(A_S)}{\Delta y} \right), \tag{7}$$

7

where $\mathbf{x}(t)$ is the animal's position at time t, $w(A_E)$, $w(A_W)$, $w(A_N)$, and $w(A_S)$ are the resource selection weightings (Equation 3) for the adjacent patches A_E, A_W, A_N and A_S in the east, west, north, and south respectively (Figure 1). We use Δx to denote the distance between the centres of patches A_E and A_W while Δy is the distance from the north patch to the south patch. Notice that, whilst there are also diagonally adjacent squares (NW, NE, SE, SW), it is sufficient to use just four to define the resource gradient, as shown in Equation (7). Then the vector $\boldsymbol{\rho}(t)$ in Equation (6) is defined as the normalised vector of $\nabla w(\mathbf{x})$,

$$\boldsymbol{\rho}(t) = \frac{\nabla w(\mathbf{x}(t))}{|\nabla w(\mathbf{x}(t))|}. \tag{8}$$

Note that we model our drift speed as constant (α) rather than letting it vary with the magnitude of $\nabla w(\mathbf{x})$. This means that the average speed of the animal across a time interval τ is kept constant, rather than being allowed to become arbitrarily large. However, the model could easily be adjusted so that $\boldsymbol{\rho}(t) = \nabla w(\mathbf{x})$ if the user believes that to be more appropriate for their particular study species.

2.1.3 Locations between observations

In each of the above movement models, we assume that the animal can potentially make a decision to reassess its movement state at any instant in continuous time. To represent this, reassessments occur according to a Poisson point process with rate κ, as in Blackwell *et al.* (2016) (see Appendix A in Supporting Information). This process means that the time intervals between reassessments are exponentially distributed with parameter κ. At each reassessment time, we deterministically decide the movement state, which is defined by either the attraction centre $\boldsymbol{\mu}(t)$ in Equation (2) or direction $\boldsymbol{\rho}(t)$ in Equation (6). The movement state is decided by comparing the relative quality of resources in different patches, using Equations (3-4), or calculating the resource gradient using Equation (7).

The fact that the choice of target location is deterministic, based on a complex evaluation of the environment, contrasts with the stochastic switching of Blackwell *et al.* (2016), where the transition rates are relatively simple functions of habitat and time. One could, in principle, extend our model so that animals choose an attraction centre with a probability, based on the relative quality of each site. However, this introduces extra model complexity that may not increase realism, so we have chosen to model a deterministic switching process for simplicity.

2.2 Inference by Markov chain Monte Carlo algorithm

Having constructed the modelling frameworks, we use a Markov chain Monte Carlo (MCMC) algorithm, based on Blackwell *et al.* (2016), to parameterise the models from movement data. For details of the algorithm, see Appendix A in Supporting Information.

The MCMC algorithm comprises two main parts, one of which updates the movement trajectory by

simulation and the other updates parameters. To take into consideration the fact that animals can make a decision to move at any time, we augment the observed data with points where the animal might have changed its destination. In every iteration, we select an interval from the observed data and generate a simulated path consisting of points where the switches of destinations might happen during the time of the selected interval. Subsequently, we compare this simulated path with the selected interval in existing trajectory by calculating the Hastings ratio, conditional on observed data points. After deciding whether to accept the proposal trajectory or not, we update the parameters conditional on the accepted trajectory (see Blackwell *et al.* (2016) for details).

2.3 Simulations

We test the MCMC algorithm on four classes of movement models. The first models migration, so we assume that the animal moves in response to seasonally changing resource qualities. In the second and third types of model, the resource quality depletes and renews according to the animal's foraging patterns. The last is a gradient-following model, where the animal only compares resource qualities in the surrounding area to decide its direction.

2.3.1 Migration model

The first test of our inference method (Section 2.2) uses a very simple model of migration, whereby the decision to migrate is a trade-off between the quality of a patch, which may be a destination range or a stopover site, and how far it is away from the animal. Although migratory routes tend to be fixed, the decision as to when to move to the next patch is not. Rather it is determined by how the quality of patches over the migratory route are changing over time (e.g. due to green-up). We hypothesise that movement to the next patch will occur when the animal will make sufficient foraging gains from the next patch to make the movement worth while. The decision to migrate is thus caused by patch quality varying over time, so we use an adjusted form of Equation (3), which includes time as a variable:

$$w(\boldsymbol{\mu}, t) = \exp(\beta_1 R(\boldsymbol{\mu}, t) + \beta_2 |\boldsymbol{\mu} - \mathbf{x}(t)|), \tag{9}$$

where $\mathbf{z}(\boldsymbol{\mu}, t) = (R(\boldsymbol{\mu}, t), |\boldsymbol{\mu} - \mathbf{x}(t)|)$ is the vector of predictor covariates with $R(\boldsymbol{\mu}, t)$ the resource quality in a potential target location $\boldsymbol{\mu}$ and $\mathbf{x}(t)$ the animal's position at time t. We assume $\beta_1 > 0$ and $\beta_2 < 0$, representing the animal's inclination for resources and aversion to distant places. Note that a similar quality/distance trade-off for patch selection was also used by Mitchell & Powell (2004) in the slightly different context of modelling home range formation.

In practice, since our aim is to use the patch that maximises Equation (9) as the movement centre, comparing the value of Equation (9) is equivalent to comparing a constant multiple of its exponent.

9

239 Moreover, we can only infer β_1/β_2 from data instead of inferring β_1 and β_2 simultaneously, because any

240 proposed values for β_1 and β_2 with ratio close to β_1/β_2 will lead to the same attraction centre. Therefore,

241 it suffices to consider a simplified version of Equation (9) as follows

$$w(\boldsymbol{\mu}, t) = \exp(\beta R(\boldsymbol{\mu}, t) - |\boldsymbol{\mu} - \mathbf{x}(t)|), \tag{10}$$

242 where $\beta = -\beta_1/\beta_2$ is termed the *resource coefficient*.

243   Our model landscape consists of N non-overlapping patches, denoted by A_i, $i \in \{1, \cdots, N\}$. The

244 centre of patch A_i is denoted by $\boldsymbol{\mu}_i = (x_i, y_i)$ with $y_1 \leq y_2 \cdots \leq y_N$, ordered by latitude. We assume the

245 resource quality changes periodically over the year and shifts corresponding to the latitude. The resource

246 quality $R(A_i, t)$ in patch A_i at time t (Julian day) is assumed to be a cosine function with period 365

247 days and shift controlled by $(y_i - y_1)/(y_N - y_1)$, the relative latitude difference:

$$R(A_i, t) = a \cos\left(\frac{2\pi}{365}t - \frac{y_i - y_1}{y_N - y_1}\pi\right) + m, \tag{11}$$

248 where a and m are the amplitude and mean of resource quality and y_i is the y-coordinate of the centre

249 of A_i (Figure 1b).

250   We generated migration trajectories by sampling from the model described above with various values

251 of the drift coefficient, b, the diffusion coefficient, v, and the resource coefficient, β in the following ranges:

252 $0.1 \leq b \leq 0.8$, $2 \leq v \leq 30$, and $1.5 \leq \beta \leq 8.5$. These are chosen to produce simulations showing migration

253 patterns on a 90×160 unit^2 landscape with 10 randomly generated non-overlapping food patches. These

254 implicitly include the winter and summer ranges and stopover sites between them.

255   We tested the MCMC algorithm on these simulations with resource qualities being given *a priori*.

256 We used a normally distributed prior for each parameter value with a mean equal to the real parameter

257 value and a standard deviation of 2. Example output is given in Figure 2a, illustrating migration from

258 the winter range in the south to the summer range in the north and back to the south over a year. We

259 used the MCMC algorithm to infer drift and diffusion coefficients (b and v respectively) from the OU

260 process in Equation (2), together with the resource coefficient, β, from the RSF in Equation (10). To

261 investigate the effectiveness of the MCMC algorithm when dealing with missing data, we carried out the

262 inference using every 5th data point, shown as red triangles in Figure 2a. We also investigated the effect

263 of finer rarification for certain simulated datasets from our study. This made very little difference to the

264 inference (details in Supplementary Appendices D-E).

2.3.2 Depletion-renewal models in a patchy landscape

266 In Section 2.3.1, we assumed that animals do not contribute in any significant way to the change of

267 resource quality (e.g. Illius *et al.* (2002)). In this section, we assume that the resource quality changes

10

according to the residential time of the animal in a food patch (e.g. Mitchell & Powell (2007), Van Moorter *et al.* (2009)). As in the migration model, we describe a situation where an animal moves in pursuit of quality food using the combination of the OU process and a RSF, introduced in Section 2.1.1. For example, this may represent how an animal forages in its home range with complete knowledge of the environment (e.g. Ford (1983)). As in Section 2.3.1, to test our inference method in a simple case, we assume that the decision to move to a patch is a trade-off between the quality of a patch and the distance to it and use the RSF given by Equation (10).

We simulate movements using Equations (2-4) in a landscape with food patches A_i, $i \in \{1, \cdots, N\}$, assuming that the resources either are consumed (if the animal is present) or renewed (otherwise). Specifically, if the animal is foraging in patch A_i at time t, that is, $\mathbf{x}(t) \in A_i$, then the resource quality $R(A_i, t)$ in patch A_i decreases exponentially while those in other patches grow logistically, so that (Ford (1983), Van Moorter *et al.* (2009))

$$R(A_j, t+\tau) = \begin{cases} R(A_j, t)e^{-d_j\tau} & \text{if } j = i, \\ \dfrac{K_j R(A_j, t)e^{r_j\tau}}{K_j + R(A_j, t)(e^{r_j\tau} - 1)} & \text{for } j \neq i, \end{cases} \tag{12}$$

where d_j, r_j and K_j are the depletion rate, growth rate and carrying capacity in patch A_j respectively and τ is a (short) time-step. For simplicity, here we assume that the growth and depletion rates and the carrying capacity are the same in each patch, and thus denoted r, d and K respectively.

We tested the inference procedure on simulations generated with various values of the drift coefficient, b, the diffusion coefficient, v, and the resource coefficient, β in the following ranges: $0.05 \leq b \leq 0.5$, $1700 \leq v \leq 3500$ and $0.5 \leq \beta \leq 5$. We used a 2000×2000 unit^2 landscape with 10 randomly generated non-overlapping food patches. Figure 2b shows an example of simulated trajectories of movements depending on resource depletion or renewal in a patchy landscape. We tested the MCMC algorithm with growth (r), depletion rate (d), and carrying capacity (K) being given. We used a normally distributed prior for each parameter value with a mean equal to the real parameter value and a standard deviation of 2. We then inferred b and v in the OU process (Equation 2) and β in Equation (10) using the Bayesian Monte Carlo algorithm. In principle, one could attempt to infer all five parameters (r, d, K, b, v) using our inference procedure, but we found that it was not usually possible to obtain precise inference in this case, so we would advise users to try to measure r, d, and K directly. An example of such a direct method is given by Fortin *et al.* (2002).

2.3.3 Depletion-renewal models in a raster landscape

Although there are many real-life situations where resource patches are disjoint and known (e.g. Merkle *et al.* (2014), Sawyer & Kauffman (2011)), often resources change continuously over the landscape and

11

are represented in data by a square grid (a.k.a. raster; e.g. Potts *et al.* (2014a)). To test whether our inference procedure is effective at determining resource attraction in such situations, we model movement on a square grid of resources that deplete and renew over time. In this case, the centre of each square in the grid is a potential attraction centre of the OU process (Equation 2).

We started each simulation with homogeneous resource type in every square, which shares the same carrying capacity, K, depletion and growth rates, d and r, across the land (e.g. Figure 2c). The initial resource quality was equal to the carrying capacity and the resource quality in time τ from time t forward was calculated using Equation (12) in Section 2.3.2. We tested our inference procedure on simulations of the model in Equations (2-4) generated with $0.05 \leq b \leq 0.14$, $0.05 \leq v \leq 0.5$ and $0.2 \leq \beta \leq 2$ on a 3×3 grid composed of unit squares. We carried out the MCMC algorithm on the assumption that d, r and K are known and attempted to infer the movement coefficients b and v in the OU process in Equation (2) and the resource coefficient β in Equation (10). As for the other simulations, we used a normally distributed prior for each parameter value with a mean equal to the real parameter value and a standard deviation of 2.

2.3.4 Gradient-following models

When landscape rasters are large, it may not be computationally feasible to test every square to see if it is an attractive centre. Instead, we take a different modelling approach, assuming that the animal tends to move up the local resource gradient, rather than towards a prime destination. This means that animals are predominantly using local perception rather than memory (cf. Bracis & Mueller (2017)). Figure 2d illustrates such a trajectory in a landscape with three different resource qualities, which are assumed to be static.

Here, the movement process is described by Equation (6) with direction corresponding to the resource gradient calculated using Equations (7) and (8). We define the RSF in Equation (7) to be the resource quality at a square. The parameters to be inferred are α and σ for the drift term and covariance matrix in Equation (6). We tested the MCMC algorithm on simulations constructed with $0.1 \leq \alpha, \sigma \leq 1$ on a 10×10 grid consisting of unit squares with 3 resource qualities. As with the other simulated trajectories, we used a normally distributed prior for each parameter value with a mean equal to the real parameter value and a standard deviation of 2. We also compared our framework with that of Hanks *et al.* (2015), testing for both inference speed and precision by application to simulated paths (details in Supplementary Appendix G). In total, for our study we analysed 45 simulated paths for the Migration model, 30 for the Patch depletion/renewal model, 30 for the Raster depletion/renewal model, and 20 for the Gradient following model.

2.4 A case study of mule deer data in the Greater Yellowstone Ecosystem

We used GPS collar data from 28 adult (> 1.5 years of age) female mule deer captured using a netgun fired from a helicopter near Cody, Wyoming (USA). Collars (ATS, Iridium, Isanti, Minnesota, USA) were programmed to take a fix every 2 hours, and we used data collected from March-August 2016. All deer were captured following protocols consistent with the University of Wyoming standards.

Before employing the MCMC inference procedure introduced in Section 2.2, we identified foraging patches by grouping data points where an animal stayed within a 3-km radius area for at least 3 days. Subsequently, the average longitude and latitude of locations inside the patches were regarded as the attraction centre (Figure 4a). For our data, these patches were quite straightforward to identify, being obvious just by looking at the location data (Figure 4a; Supplementary Video SV1), and the deer have high fidelity to these sites (Sawyer & Kauffman, 2011). However, this may not be true for all datasets on migratory movement. For each attraction centre, we extracted the values of the normalised difference vegetation index (NDVI) and instantaneous rate of green-up (IRG) for Julian days 1 to 250 from the corresponding pixels in the images (Figures 4c). NDVI and IRG data were compiled from the MODIS satellite based on the methods of Bischof et $al.$ (2012) and Merkle et $al.$ (2016).

Our model is based on Equation (10) for decision making and the OU process in Equation (2) for movement, and can be written out in full as follows

$$\mathbf{x}(t + \tau)|\mathbf{x}(t) \sim MVN(\boldsymbol{\mu}(t) + e^{-b\tau}(\mathbf{x}(t) - \boldsymbol{\mu}(t)), vI(1 - e^{-2b\tau})), \tag{13}$$

$$\boldsymbol{\mu}(t) = \mathrm{argmax}_{i \in \Omega}[\exp(\beta R(\boldsymbol{\mu}_i, t) - |\boldsymbol{\mu}_i - \mathbf{x}(t)|)], \tag{14}$$

where Ω indexes the set of attraction centres (centres of the foraging patches). We used our MCMC algorithm to parameterise two different models from data. The first was the NDVI Model, where $R(\boldsymbol{\mu}_i, t)$ is the NDVI value of patch i at time t. The second was the IRG Model, where $R(\boldsymbol{\mu}_i, t)$ is the IRG value of patch i at time t. We used the Deviance Information Criterion (DIC) (Spiegelhalter et $al.$ (2002)) for model selection.

3 Results

3.1 Testing MCMC inference on simulations

3.1.1 Migration model

Figure 3a shows the posterior distributions derived by applying MCMC inference on the trajectory shown in Figure 2a. The posterior distributions captured the real values of parameters used in simulations to a good degree of accuracy with the real values lying within a 95% quantile interval of the posterior distributions, indicated by black dashed lines in Figure 3a.

When applying the MCMC algorithm on the migration model, the sampling chains converged within similar numbers of iteration in about 20 minutes (on a single thread of an i5 2.0GHz processor in a Windows desktop) regardless of various values for parameters used in simulation (Figure S1 in the Supporting Information). It took longer for the chains to converge when the number of proposed switching points increases (Figure S2a,b). However, the performance of estimation was not affected by the amount of proposed points (Figure S2c-e). Although the value of increasing κ was insignificant here, it might become important when the frequency of state switch is much higher than observation.

As one would expect, the chains converged faster when the initial value of the drift coefficient, b, was closer to the real value, in cases when the diffusion coefficient, v, and the resource coefficient, β, were fixed at real values (Figures S3a,b). However, the initial value of v had little impact on converging time (Figures S3c,d), while the chains converged faster when the initial value of β was near the real value (Figures S3e,f).

As for accuracy, the real values of b, v and β were within 95% central posterior intervals of the estimated values for about 2/3, 4/5 and 1/2 simulations respectively (Figure S4, Table S1). (See Appendices B, F in Supporting Information for more details.) However, where they did deviate from these intervals the deviations were generally quite small (a discrepancy of less than about 25% in all cases).

3.1.2 Resource depletion-renewal models in a patchy landscape

The 95% central posterior interval of each posterior distribution in Figure 2b contains the real values (Figure 3b), showing that our inference procedure has good accuracy in this case.

The algorithm was able to converge within 26,000 iterations (approximately 55 minutes) in most cases (Figure S5 in the Supporting Information). It took longer for the chains to converge when the initial value of b was far away from the real value, whereas the initial values of v and β had little influence on the time before converging (Figure S6). While b and v were captured by 95% central posterior intervals for most cases, β was overestimated when the values of v or β used in simulations were higher (Figure S7, Table S1) (See Appendix C in Supporting Information for more details.)

14

3.1.3 Resource depletion-renewal models in a raster landscape

For the case shown in Figure 2c, the posterior distributions captured parameters successfully, as shown in Figure 3c, despite that it is not straightforward to identify the attraction centres simply by eyeballing the trajectory.

In general, the convergence time of the algorithm was independent of the values of coefficients used in simulations (Figures S8 in the Supporting Information). However, starting the algorithm with initial values closer to real values usually led to faster convergence, as one would expect (Figure S9).

The performance of the MCMC algorithm using every 5th data point was similar to that using every 3rd point, but the discrepancy between sample means of β and real values was lower when more observations were considered (Figures S10,11,12). (See Appendix D in Supporting Information for more details.)

3.1.4 Gradient-following models

In the case shown in Figure 2d, the posterior distributions successfully captured the real values within 95% central posterior intervals.

The value of the drift speed, α, used to generate a simulated trajectory had no obvious impact on the time when MCMC chains converged (Figure S13a in the Supporting information). On the other hand, the chains tended to converge quicker when larger σ was used in simulation (Figure S13b). There was no clear relationship between the convergence time and initial values for the MCMC algorithm when inferring parameters from the simulation in Figure 2d (Figure S14). Initial values near real values did not guarantee faster convergence. On the contrary, the algorithm converged after fewer iterations when the initial values of α were more than 10 times larger than the real value (Figure S14b). This might result from the slower convergence of the sampling chain of σ, which dominated the overall converging time, and fluctuations in the chains caused by the augmentation of data points. In general, the accuracy of estimating σ improved significantly when more data points were used in the inference procedure, while the accuracy of estimating α was less affected by the density of data (Figures S15,16). (See Appendix E in Supporting Information for more details.) Our comparison with the method of Hanks *et al.* (2015) reveals that our method shows that our method is more precise (e.g. the posterior standard deviation of α was more than an order of magnitude smaller than the equivalent measure from the model of Hanks *et al.* (2015)) on data simulated from our model.

3.2 Applying MCMC inference on the mule deer data

When fitting the IRG Model to the deer data, the MCMC algorithm converged for 27 of the 28 individuals, whereas the NDVI Model only converged for 9. This gives some preliminary indication that the NDVI

15

model is not a good model for these data. In the 9 cases where both the NDVI and IRG Models led to convergent MCMC results (e.g. No. 4, Table 1), the DIC was used to determine the better model. This reveals that the NDVI Model is a better fit for one of the deer (No. 10) and the IRG Model for the other eight (Table 1), confirming our preliminary indications. For those cases where MCMC chains converged, we used the posterior mean of β of the best fit model to calculate the simulated departure dates of migration, shown together with the real departure dates in Table 1. The estimated departure dates were defined to be the dates when a switch of movement centre had occurred according to the RSF. The observed departure dates were the dates when locations occurring outside a patch and towards another patch were first observed. The agreement was generally good, suggesting that, when a model can be fitted to the data, the timing of migration can be explained by a simple trade-off between relative NDVI or IRG values and the distance between successive patches, but usually IRG is a better measurement to use (Figure 5).

However, for one individual (No. 21, Table 1), the inference procedure estimated that the individual left a patch, and was attracted to it again for a very short time soon after migrating. This is probably not a behavioural feature, though, since it was not observed in the data. Rather, this is likely to be a quirk resulting from small up-and-down fluctuation in the IRG around the time of migration.

Figure 4a gives an example migratory path of an individual, which can be compared with the simulated path from the best-fit model (Figure 4b). Supplementary Video SV1 shows an animation of both these paths superimposed (red dots are the observed locations and blue are simulated). In the best-fit model, the attraction centre changed from $\boldsymbol{\mu}_1$ to $\boldsymbol{\mu}_2$ on the 126th day of the year (Table 1). This is very close to the actual date of departure from winter range observed from data and is marked by an arrow in Figure 4c. Finally, the posterior distributions for this example are given in Figure 4d, where we observe a significant difference between the posterior mean and zero for each parameter ($p < 10^{-5}$).

4 Discussion

We have constructed models of resource selection in continuous time, based on a switching random walk process, and parameterised using a Bayesian Monte Carlo algorithm. We have demonstrated that our method can be applied in a wide range of scenarios, including both movements driven by the evaluation of resources at the landscape scale, and those that simply follow local resource gradients. In broad terms, our model animals first (a) assess location and quality of different resources (either proximately or across the whole landscape), to decide the general direction of movement, then (b) move according to a process that incorporates not only the resource-based decision, but also some stochasticity to account for any unknown factors governing movement. Such stochastic continuous-time models allow us to make use of well-developed, flexible inference procedures (Blackwell *et al.* (2016)). When applying our inference

16

No.	simulated departure date (the NDVI Model)	simulated departure date (the IRG Model)	observed departure date	ΔDIC
4	128	**126**	125	167.58
6	138	**134**	133	117.25
10	**124,132**	124, 132	123,128	141.79
11	127,152	**126, 151**	125,149	182.79
13	148	**142**	140	75.53
18	130,158	**124,158**	123,157	97.84
20	135,146	**134,146**	133,145	54.27
21	152	**149,150,150**	144	185.09
25	142	**141**	140	496.41
1	–	100,151	132,150	
2	–	153	147	
3	–	126,158	125,154	
5	–	143	142	
7	–	151	148	
8	–	157	154	
9	–	147	144	
12	–	146	140	
14	–	140	139	
15	–	149	139	
16	–	101,138,148	112,136,147	
17	–	142	139	
22	–	149	146	
23	–	134	133	
24	–	140	139	
26	–	125,141	124,137	
27	–	148	128	
28	–	134	131	

Table 1: The comparison of models for the mule deer data. For cases where the switch of movement centre occurred on two days, the numbers for the Julian dates are separated with a comma. Figures in bold indicate the model with smaller DIC value on that individual.

algorithm to simulated data, where all the parameter values governing the movement are known, we were able to estimate the input parameters, including those governing the trade-off between maximising resource intake and minimising travel costs, with good accuracy. As such, our method can reliably capture important aspects of the processes underlying movement decisions.

Our framework can be viewed as generalising ideas from several previous studies. The study of Hanks *et al.* (2015) developed a gradient following algorithm that allows for behavioural switches between observed locations. This is similar to our gradient-following model, yet relies upon discretising the path into presence or absence on pixels of a square lattice, whereas ours considers the full, continuous path. A comparison of our method with that of Hanks *et al.* (2015) on a path simulated from our model revealed that in this case our method is more precise. However, this is not surprising, as we would expect a better fit from a model that accurately mimics the true movement process. Employing the model in Hanks *et al.* (2015), Brennan *et al.* (2018) attempted better understanding of habitat preferences by considering the impact of corridor choice on speed during migration, while we focus on the movement direction decided by identifying the destination. Breed *et al.* (2017) gives a model of patch-to-patch movement, based on a switching OU process, but where only the decision to *leave* a patch depends on environmental features. Ours generalises this by modelling patch-to-patch movements as dependent on the source patch, the target patch, and the distance between them.

In this study, we have examined gradient-following and patch selection models separately. In principle, it would be possible to combine these. One would begin by writing down a stochastic differential equation that combines the processes in Equations (1) and (5) then derive from these the distribution of movement across a short time-interval (similar to Equations 2 and 6). This distribution can then be fed into the inference algorithm described in Section 2.2. Of course, such a model would be more complex than those described here, so would likely require more running time and a good dataset to achieve accurate inference.

We have focused on a few simple situations where the main factor in movement decisions is resource quality. However, being based on a resource selection function (RSF), our framework has potential to incorporate as wide a variety of movement covariates as in traditional resource- or step-selection analysis. For example, topography (Potts *et al.* (2014c)), interactions between animals (Vanak *et al.* (2013)), memory effects (Merkle *et al.* (2017)), barriers and corridors (Panzacchi *et al.* (2016)) have all been incorporated into step-selection analysis and so could, in principle, be incorporated into our modelling framework.

Classical step selection analysis tends to examine resource selection from one measured location to the next (Thurfjell *et al.* (2014)). However, it has occasionally been used to measure patch-to-patch movements (e.g. Merkle *et al.* (2014)) and this is similar in flavour to our patch-based models. On the other hand, our raster-based models are more appropriate for studies where distinct patches are less

18

clear. In this case, it is often far less clear what spatio-temporal scales are being used by the animal to make selection decisions. However, to use step selection analysis, one is forced either to make an *a priori* choice of scale or perform a complicated model selection procedure (Bastille-Rousseau *et al.* (2018)). Our approach has the advantage that the spatio-temporal scale of decision-making emerges from the interface between the landscape and the movement processes, and is not tied to the frequency of the location data. In addition, the flexibility of the switching random walk framework means that our models have potential to include variation in behavioural modes in different parts of space (Harris & Blackwell (2013)) or in different states such as encamped and exploratory states (Morales *et al.* (2004)).

Indeed, the switching OU framework used here has recently been used to model state-switching correlated random walks (Michelot & Blackwell (2019)). This makes use of the same code base as the code used for inference here, so is ready to be combined with our models. Furthermore, although we have developed our techniques for use with single animal tracks, there is ongoing work to incorporate collective movement and animal interactions into the switching OU framework (Niu *et al.* (2016)), which could be important for the study of mule deer (Sawyer *et al.*, 2006). Therefore we intend for future studies to factor group movement into continuous-time resource selection.

To demonstrate how our techniques can be applied to real data, we assessed the underlying mechanisms behind migration in mule deer. Our results support two hypotheses related to migration. First is the Forage Maturation Hypothesis, which posits that as plants grow herbivores face a trade-off between forage quality and quantity and therefore will select forage patches at intermediate stages of growth (Fryxell (1991), Hebblewhite *et al.* (2008)). Second is the Green Wave Hypothesis (Drent *et al.* (1978)), which is the spatial manifestation of the Forage Maturation Hypothesis (Merkle *et al.* (2016)). The Green Wave Hypothesis posits that animals migrate to acquire high-quality foods that are propagated as resource waves in space and time. For migratory herbivores, resource waves often correspond to the onset of spring along the migration route (Aikens *et al.* (2017)). The Green Wave Hypothesis has been tested in a variety of species of both birds and mammals (van Wijk *et al.* (2012), Kölzsch *et al.* (2015), Merkle *et al.* (2016)).

We used a model where the animal trades-off the relative quality of resources at source and target locations with the effort of moving from one to the other (using distance between patches as a proxy for effort). We used two proxies for resource quality of a patch: NDVI and IRG. The former represents an index of green forage biomass, and the latter represents an index of intermediate forage biomass (Bischof *et al.* (2012)). Similar to the findings of Aikens *et al.* (2017) and Merkle *et al.* (2016) for mule deer, our results suggest that the movements of most individual mule deer could be explained by IRG. The use of growth *rate* (IRG), rather than *absolute* quality of biomass (NDVI) suggests that movement is caused predominantly by the *process* of change, i.e. green-up. This is consistent with the idea of 'surfing a green wave': tracking the places at which rate of change is greatest. Note that for one individual, however,

19

the model using NDVI did fit better (No. 10, Table 1). Nonetheless, the resulting best-fit models tend to anticipate the migratory times well (Table 1, Figure 5), and simulated paths are qualitatively similar to the real paths (Supplementary Video SV1). Therefore our method has potential to test various hypotheses explaining migratory movement, and resource-driven movement in general.

In conclusion, we have developed a flexible framework for continuous-time inference of resource selection decisions in moving animals. The switching random-walk model, combined with Bayesian Monte Carlo inference, generalises several previous methods, and has potential to be extended to a wide range of scenarios. Whilst the inference speed is sufficient for paths of several hundred data-points, it may prove too slow with modern-era tracks that can contain millions (Hays *et al.* (2016)). Therefore a significant future challenge would be to develop either methods for speeding-up inference significantly (Kálmán filters may be an appropriate technique here: e.g. Fleming *et al.* (2017)), or rarefying high-resolution data to extract key locations in the path that represent animal decisions (Potts *et al.* (2018)). Indeed, the key limiting factor for speed is the number of MCMC samples required for convergence. Better data, sampled at behaviourally-meaningful locations, may have a clearer signal thus requiring less time for the MCMC procedure to converge, even if the datasets might be larger. In summary, our framework represents an important methodological step in understanding resource-use decisions by moving animals.

Acknowledgements

Author Contributions

JRP, PGB conceived and designed the research; YW performed the research; JAM provided data; PGB provided code for inference; YW, JRP led the writing of the manuscript. All authors contributed critically to the drafts and gave final approval for publication.

Data Accessibility

Data used in this manuscript are archived on Data Dryad at `doi:10.5061/dryad.f9p3dq4`.

References

1.

Aikens, E.O., Kauffman, M.J., Merkle, J.A., Dwinnell, S.P., Fralick, G.L. & Monteith, K.L. (2017). The greenscape shapes surfing of resource waves in a large migratory herbivore. *Ecol. Lett.*, 20, 741–750.

2.

Avgar, T., Lele, S.R., Keim, J.L. & Boyce, M.S. (2017). Relative Selection Strength: Quantifying effect size in habitat- and step-selection inference. *Ecol Evol*, 7, 5322–5330.

3.

Avgar, T., Potts, J.R., Lewis, M.A. & Boyce, M.S. (2016). Integrated step selection analysis: bridging the gap between resource selection and animal movement. *Methods Ecol Evol*, 7, 619–630.

4.

Bastille-Rousseau, G., Murray, D.L., Schaefer, J.A., Lewis, M.A., Mahoney, S.P. & Potts, J.R. (2018). Spatial scales of habitat selection decisions: implications for telemetry-based movement modelling. *Ecography*, 41, 437–443.

5.

Bastille-Rousseau, G., Potts, J.R., Schaefer, J.A., Lewis, M.A., Ellington, E., Rayl, N., Mahoney, S. & Murray, D.L. (2015). Unveiling trade-offs in resource selection of migratory caribou using a mechanistic movement model of availability. *Ecography*, 38, 1049–1059.

6.

Bischof, R., Loe, L.E., Meisingset, E.L., Zimmermann, B., Van Moorter, B. & Mysterud, A. (2012). A migratory northern ungulate in the pursuit of spring: jumping or surfing the green wave? *Am. Nat.*, 180, 407–424.

7.

Blackwell, P.G. (1997). Random diffusion models for animal movement. *Ecol Modell*, 100, 87–102.

8.

Blackwell, P.G. (2003). Bayesian inference for Markov processes with diffusion and discrete components. *Biometrika*, 90, 613–627.

9.

Blackwell, P.G., Niu, M., Lambert, M.S. & LaPoint, S.D. (2016). Exact Bayesian inference for animal movement in continuous time. *Methods Ecol Evol*, 7, 184–195.

10.

Boyce, M.S. (2006). Scale for resource selection functions. *Diversity Distrib.*, 12, 269–276.

11.

Boyce, M.S., Vernier, P.R., Nielsen, S.E. & Schmiegelow, F.K. (2002). Evaluating resource selection functions. *Ecol Modell*, 157, 281–300.

12.

Bracis, C. & Mueller, T. (2017). Memory, not just perception, plays an importnat role in terrestrial mammalian migration. *Proc. R. Soc. B*, 284, 20170449.

13.

Breed, G.A., Golson, E.A. & Tinker, M.T. (2017). Predicting animal home-range structure and transitions using a multistate Ornstein-Uhlenbeck biased random walk. *Ecology*, 98, 32–47.

14.

Brennan, A., Hanks, E.M., Merkle, J.A., Cole, E.K., Dewey, S.R., Courtemanch, A.B. & Cross, P.C. (2018). Examining speed versus selection in connectivity models using elk migration as an example. *Landscape Ecol*, 33, 955–968.

15.

Cagnacci, F., Boitani, L., Powell, R.A. & Boyce, M.S. (2010). Animal ecology meets GPS-based radiotelemetry: a perfect storm of opportunities and challenges. *Phil. Tran. R. Soc. B*, 365, 2157–2162.

16.

Chetkiewicz, C.L.B. & Boyce, M.S. (2009). Use of resource selection functions to identify conservation corridors. *J. Appl. Ecol.*, 46, 1036–1047.

17.

Drent, R., Ebbinge, B. & Weijand, B. (1978). Balancing the energy budgets of arctic-breeding geese throughout the annual cycle: a progress report. *Verh. Ornithol. Ges. Bayern.*, 23, 239–264.

18.

Fleming, C.H., Sheldon, D., Gurarie, E., Fagan, W.F., LaPoint, S. & Calabrese, J.M. (2017). Kálmán filters for continuous-time movement models. *Ecol. Inform.*, 40, 8–21.

19.

Ford, R.G. (1983). Home range in a patchy environment: optimal foraging predictions. *Integr. Comp. Biol.*, 23, 315–326.

20.

Forester, J., Im, H. & Rathouz, P. (2009). Accounting for animal movement in estimation of resource selection functions: sampling and data analysis. *Ecology*, 90, 3554–3565.

21.

Fortin, D., Beyer, H., Boyce, M.S., Smith, D., Duchesne, T. & Mao, J.S. (2005). Wolves influence elk movements: behavior shapes a trophic cascade in Yellowstone National Park. *Ecology*, 86, 1320–1330.

22.

Fortin, D., Fryxell, J.M. & Pilote, R. (2002). The temporal scale of foraging decisions in bison. *Ecology*, 83, 970–982.

23.

Fryxell, J.M. (1991). Forage quality and aggregation by large herbivores. *Am. Nat.*, 138, 478–498.

24.

Hanks, E.M., Hooten, M.B. & Alldredge, M.W. (2015). Continuous-time discrete-space models for animal movement. *Ann. Appl. Stat.*, 9, 145–165.

25.

Hanks, E.M., Hooten, M.B., Johnson, D.S. & Sterling, J.T. (2011). Velocity-based movement modeling for individual and population level inference. *PLOS ONE*, 6, e22795.

26.

Harris, K.J. & Blackwell, P.G. (2013). Flexible continuous-time modelling for heterogeneous animal movement. *Ecol Modell*, 255, 29–37.

27.

Hays, G., Ferreira, L., Sequeira, A., Meekan, M., Duarte, C., Bailey, H., Bailleul, F., Bowen, W., Caley, M. & Costa, D. (2016). Key questions in marine megafauna movement ecology. *Trends Ecol. Evol.*, 31, 463–475.

28.

Hebblewhite, M., Merrill, E. & McDermid, G. (2008). A multi-scale test of the forage maturation hypothesis in a partially migratory ungulate population. *Ecol. Monogr.*, 78, 141–166.

29.

Hooten, M.B., Johnson, D.S., Hanks, E.M. & Lowry, J.H. (2010). Agent-based inference for animal movement and selection. *J Agric Biol Environ Stat*, 15, 523–538.

30.

Illius, A.W., Duncan, P., Richard, C. & Mesochina, P. (2002). Mechanisms of functional response and resource exploitation in browsing roe deer. *J. Anim. Ecol.*, 71, 723–734.

31.

Johnson, D.S., Thomas, D.L., Ver Hoef, J.M. & Christ, A. (2008). A general framework for the analysis of animal resource selection from telemtry data. *Biometrics*, 64, 968–976.

32.

Kölzsch, A., Bauer, S., Boer, R., Griffin, L., Cabot, D., Exo, K.M., van der Jeugd, H.P. & Nolet, B.A. (2015). Forecasting spring from afar? Timing of migration and predictability of phenology along different migration routes of an avian herbivore. *J. Anim. Ecol.*, 84, 272–283.

33.

Lendrum, P.E., Anderson Jr., C.R., Long, R.A., Kie, J.G. & Bowyer, R.T. (2012). Habitat selection by mule deer during migration: effects of landscape structure and natural-gas development. *Ecosphere*, 3, 82.

34.

Manly, B., McDonald, L., Thomas, D., McDonald, T. & Erickson, W. (2002). *Resource selection by animals: statistical analysis and design for field studies*. 2nd edn. Springer Netherlands.

35.

McClintock, B.T., Johnson, D.S., Hooten, M.B., Ver Hoef, J.M. & Morales, J.M. (2014). When to be discrete: the importance of time formulation in understanding animal movement. *Movement Ecol*, 2.

36.

McLoughlin, P.D., Morris, D.W., Fortin, D., Vander Wal, E. & Contasti, A.L. (2010). Considering ecological dynamics in resource selection functions. *J. Anim. Ecol.*, 79, 4–12.

37.

Merkle, J.A., Cross, P., Scurlock, B.M., Cole, E., Courtemanch, A., Dewey, S. & Kauffman, M.J. (2018). Linking spring phenology with mechanistic models of host movement to predict disease transmission risk. *J. Appl. Ecol.*, 55, 810–819.

38.

Merkle, J.A., Fortin, D. & Morales, J.M. (2014). A memory-based foraging tactic reveals an adaptive

mechanism for restricted space use. *Ecol Lett*, 17, 924–931.

39.

Merkle, J.A., Monteith, K.L., Aikens, E.O., Hayes, M.M., Hersey, K.R., Middleton, A.D., Oates, B.A.,

Sawyer, H., Scurlock, B.M. & Kauffman, M.J. (2016). Large herbivores surf waves of green-up during

spring. *Proc. R. Soc. B*, 283, 20160456.

40.

Merkle, J.A., Potts, J.R. & Fortin, D. (2017). Energy benefits and emergent space use patterns of an

empirically parameterized model of memory-based patch selection. *Oikos*, 126.

41.

Michelot, T. & Blackwell, P.G. (2019). State-switching continuous-time correlated random walks.

Methods in Ecology and Evolution.

42.

Michelot, T., Blackwell, P.G. & Matthiopoulos, J. (2018). Linking resource selection and step selection

models for habitat preferences in animals. *Ecology*. Accepted Author Manuscript.

43.

Mitchell, M.S. & Powell, R.A. (2004). A mechanistic home range model for optimal use of spatially

distributed resources. *Ecol. Modell.*, 177, 209–232.

44.

Mitchell, M.S. & Powell, R.A. (2007). Optimal use of resources structures home ranges and spatial

distribution of black bears. *Anim. Behav.*, 74, 219–230.

45.

Moorcroft, P. & Barnett, A. (2008). Mechanistic home range models and resource selection analysis:

a reconciliation and unification. *Ecology*, 89, 1112–1119.

46.

Morales, J.M., Haydon, D.T., Frair, J., Holsinger, K.E. & Fryxell, J.M. (2004). Extracting more out

of relocation data: building movement models as mixtures of random walks. *Ecology*, 85, 2436–2445.

47.

Niu, M., Blackwell, P.G. & Skarin, A. (2016). Modeling interdependent animal movement in continuous

time. *Biometrics*, 72, 315–324.

48.

Panzacchi, M., Van Moorter, B., Strand, O., Saerens, M., Kivimäki, I., St. Clair, C.C., Herfindal, I. & Boitani, L. (2016). Predicting the *continuum* between corridors and barriers to animal movements using Step Selection Functions and Randomized Shortest Paths. *J. Anim. Ecol.*, 85, 32–42.

49.

Potts, J.R., Bastille-Rousseau, G., Murray, D.L., Schaefer, J.A. & Lewis, M.A. (2014a). Predicting local and non-local effects of resources on animal space use using a mechanistic step selection model. *Methods Ecol Evol*, 5, 253–262.

50.

Potts, J.R., Börger, L., Scantlebury, D.M., Bennett, N.C., Alagaili, A. & Wilson, R.P. (2018). Finding turning-points in ultra-high-resolution animal movement data. *Methods Ecol. Evol.*, Accepted Author Manuscript.

51.

Potts, J.R., Mokcross, K. & Lewis, M.A. (2014b). A unifying framework for quantifying the nature of animal interactions. *J. R. Soc. Interface*, 11, 20140333.

52.

Potts, J.R., Mokcross, K., Stouffer, P. & Lewis, M.A. (2014c). Step selection techniques uncover the environmental predictors of space use patterns in flocks of amazonian birds. *Ecol Evol*, 4, 4578–4588.

53.

Preisler, H.K., Ager, A.A., Johnson, B.K. & Kie, J.G. (2004). Modeling animal movements using stochastic differential equations. *Environmetrics*, 15, 643–657.

54.

Preisler, H.K., Ager, A.A. & Wisdom, M.J. (2013). Analyzing animal movement patterns using potential functions. *Ecosphere*, 4, 1–13.

55.

Sawyer, H. & Kauffman, M.J. (2011). Stopover ecology of a migratory ungulate. *J. Anim. Ecol.*, 80, 1078–1087.

56.

Sawyer, H., Nielson, R.M., Lindzey, F. & McDONALD, L.L. (2006). Winter habitat selection of mule deer before and during development of a natural gas field. *The Journal of Wildlife Management*, 70, 396–403.

729   57.

730   Spiegelhalter, D.J., Best, N.G., Carlin, B.P. & Van Der Linde, A. (2002). Bayesian measures of model

731   complexity and fit. *Journal of the Royal Statistical Society: Series B (Statistical Methodology)*, 64,

732   583–639.

733   58.

734   Thurfjell, H., Ciuti, S. & Boyce, M.S. (2014). Applications of step-selection functions in ecology and

735   conservation. *Movement Ecol*, 2, 4.

736   59.

737   Van Moorter, B., Visscher, D., Benhamou, S., Börger, L., Boyce, M.S. & Gaillard, J.M. (2009).

738   Memory keeps you at home: a mechanistic model for home range emergence. *Oikos*, 118, 641–652.

739   60.

740   Vanak, A., Fortin, D., Thakera, M., Ogdene, M., Owena, C., Greatwood, S. & Slotow, R. (2013).

741   Moving to stay in place - behavioral mechanisms for coexistence of african large carnivores. *Ecology*,

742   94, 2619–2613.

743   61.

744   van Wijk, R.E., Kölzsch, A., Kruckenberg, H., Ebbinge, B.S., Müskens, G.J. & Nolet, B.A. (2012).

745   Individually tracked geese follow peaks of temperature acceleration during spring migration. *Oikos*,
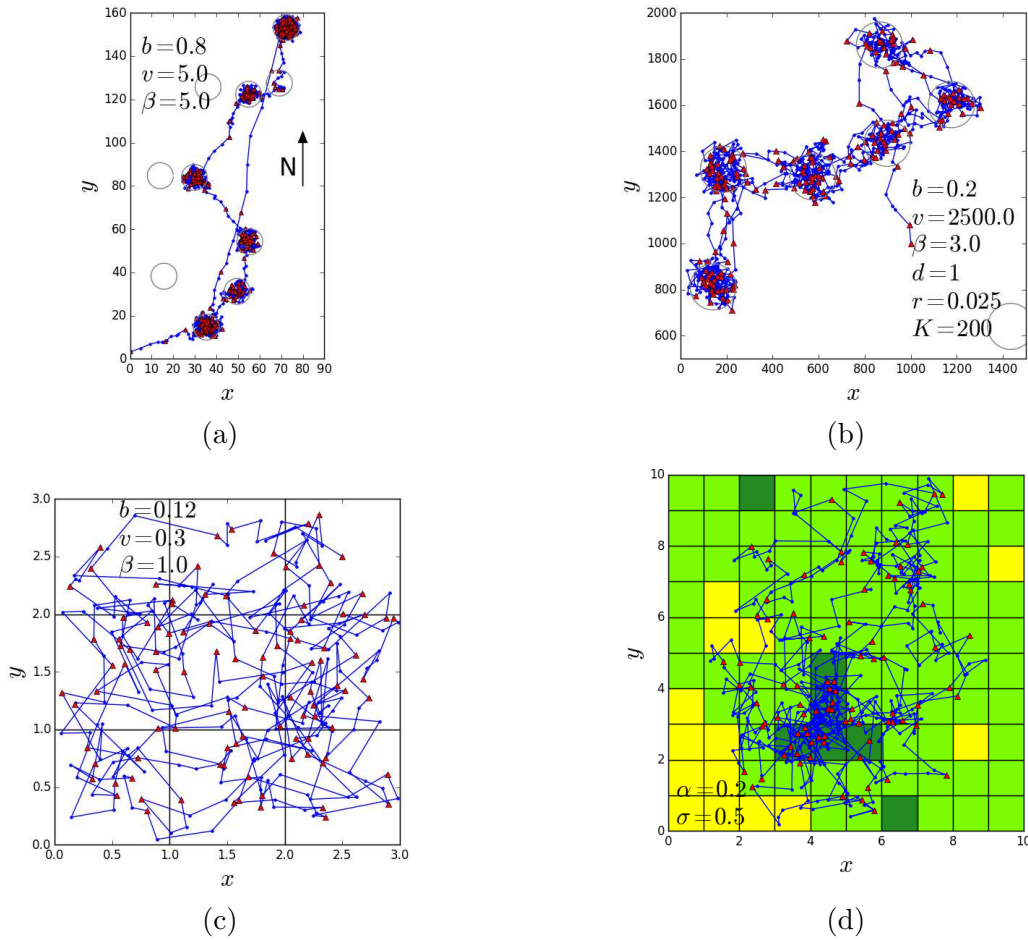
746   121, 655–664.

Figure 2: Simulations corresponding to (a) the Migration model (Section 2.3.1), (b) the Patch depletion/renewal model (Section 2.3.2), (c) the Raster depletion/renewal model (Section 2.3.3), and (d) the Gradient following model (Section 2.3.4). The blue dots and line segments show the whole set of data points, and the red triangles are those used in the MCMC algorithm. (a) A simulated trajectory of migration during one year using the OU process in Equation (2) and RSF in Equation (10) with resource quality in Equation (11). The animal moves towards the north from patches in the south and comes back to the south. (b) A simulated trajectory in a patchy landscape with the resource depletion-renewal model. The resource quality changes according to Equation (12) and the movement process is given by Equations (2) and (10). (c) A simulated trajectory in a homogeneous raster landscape with the resource depletion-renewal model. The resource quality changes according to Equation (12) and the movement process is given by Equations (2) and (10). (d) A simulation of movement following resource gradient, according to Equations (6) and (7). The different colours in the landscape represent different resource types. Dark green, light green and yellow stand for high, medium and low resource quality respectively.
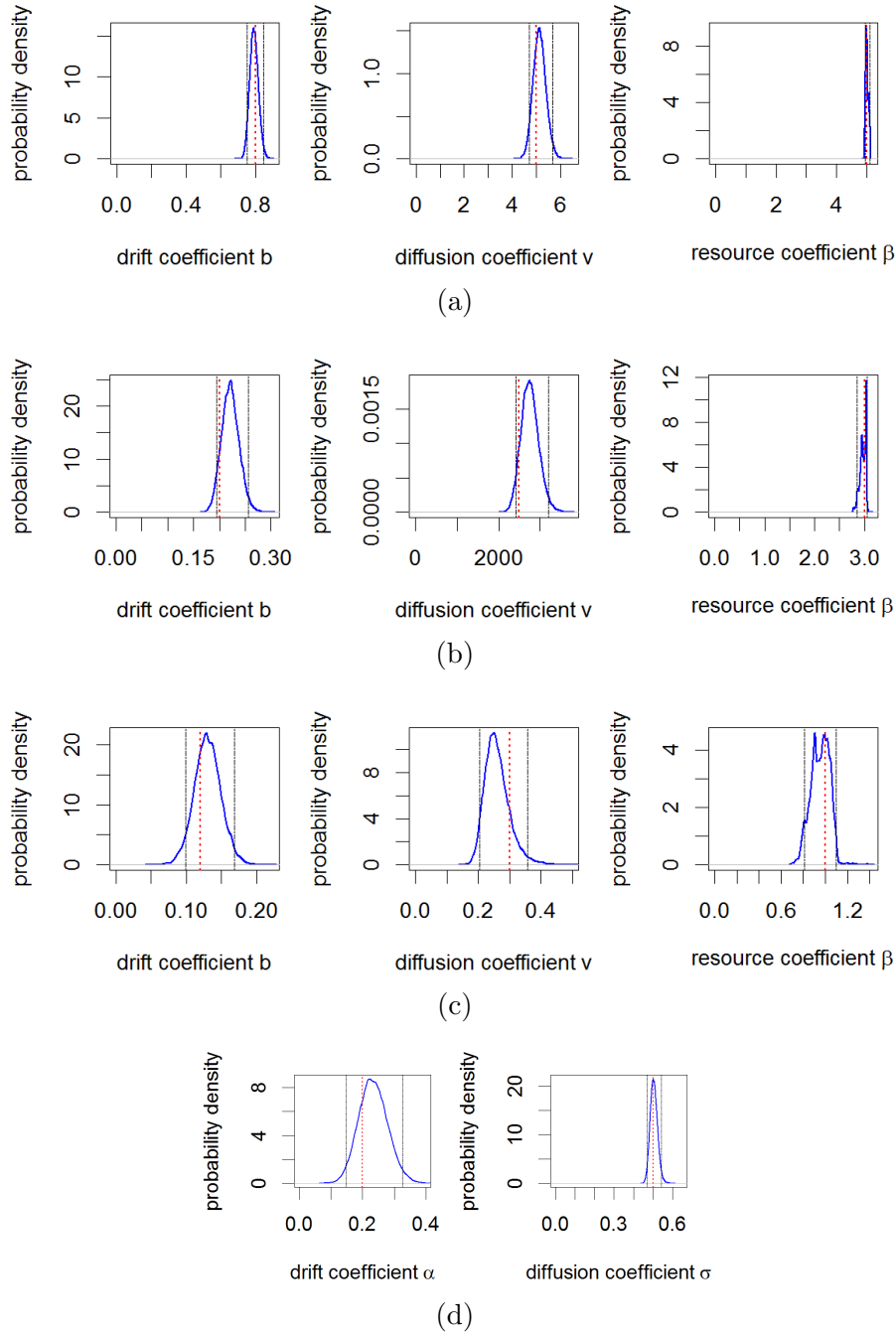
Figure 3: Posterior distributions of parameters obtained by applying the MCMC inference procedure to the simulationed trajectories in Figure 2. Red dotted lines indicate real values used in simulations and black dashed lines shows 95% quantile intervals. Panel (a) uses the Migration model (Figure 2a). Panel (b) uses the Patch depletion/renewal model (Figure 2b). Panel (c) uses the Raster depletion/renewal model (Figure 2c). Each of (a-c) show the inferred posterior distributions of the movement coefficients, b and v, from Equation (2) and the resource coefficient, β, from Equation (10). Panel (d) uses the Gradient following model (Figure 2d) and shows the posterior distribution of the drift and diffusion coefficients (α and σ, respectively) from Equation (6).
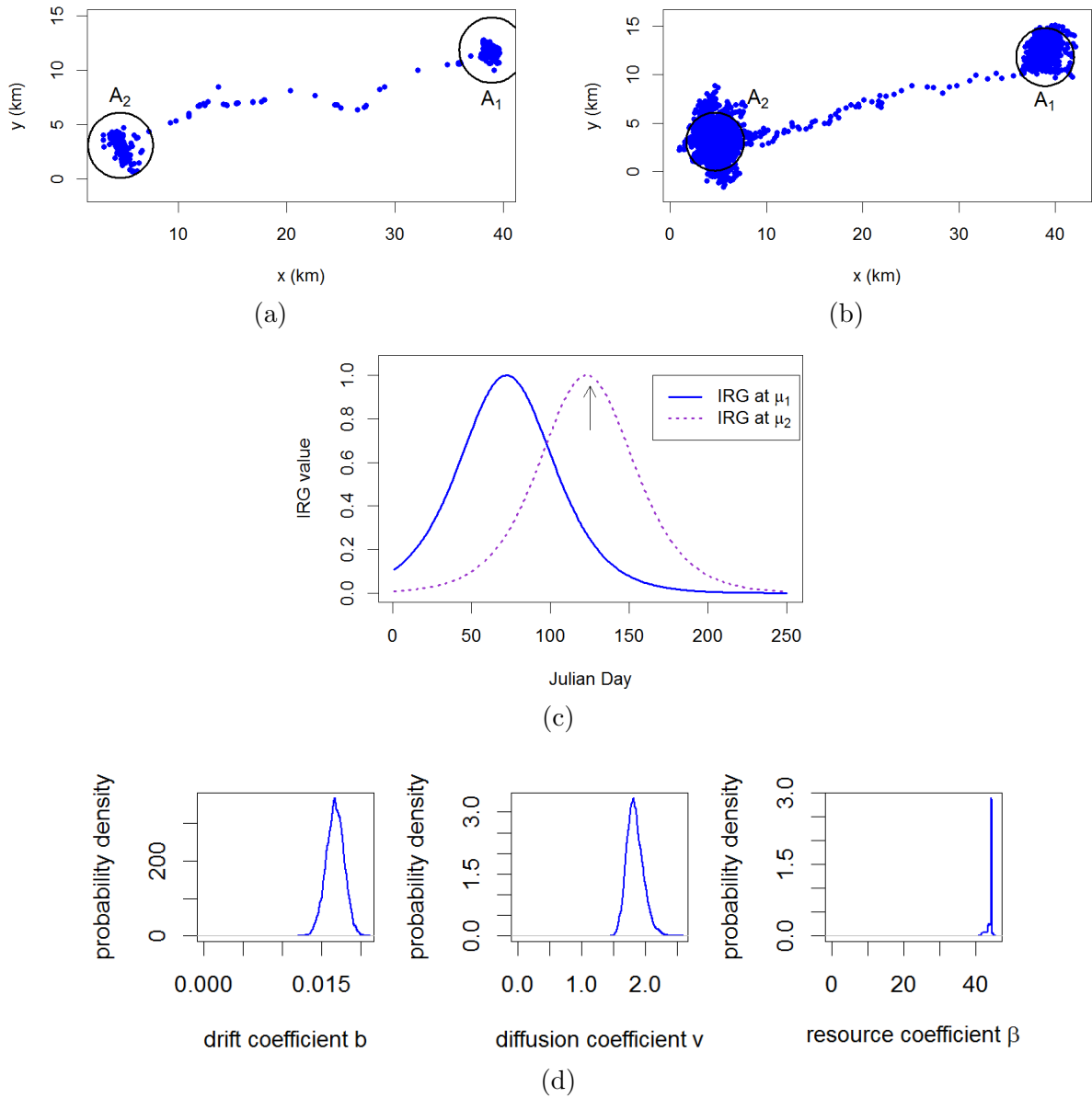
Figure 4: A case study of mule deer data. (a) The migration trajectory of mule deer No. 4. The blue dots are observed locations collected between March and August 2016. The circles A_1 and A_2 are foraging patches where the mule deer spent more than two weeks. (b) A simulated trajectory of mule deer migration, generated using posterior means derived from analysing the data of deer No. 4 with the IRG model. (c) The IRG values at μ_1 and μ_2, the centres of patches A_1 and A_2 illustrated in Figure 4a. The arrow indicates the date when the mule deer left patch A_1. (d) The posterior distributions derived by applying the MCMC algorithm on the trajectory of mule deer No. 4, shown in Figure 4a, with the IRG model.
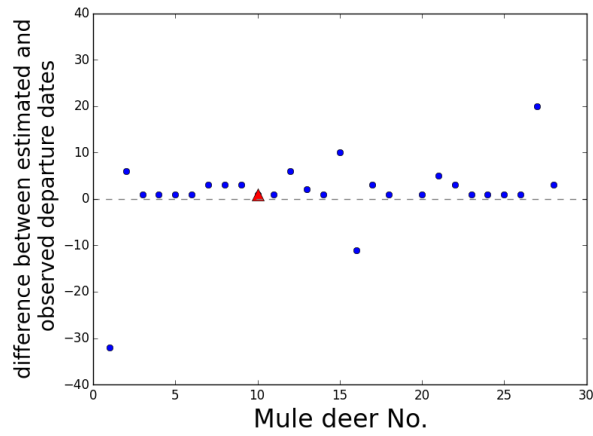
Figure 5: A comparison between the estimated and observed dates when leaving winter ranges. Blue dots show the cases where the IRG Model fitted the data better, while the red triangle represents the case where the NDVI Model was better (No. 10, Table 1). Markers above and below the horizontal dashed line indicate that the estimated departure date was later and earlier than the observed date respectively.